Eng. & Tech. Journal, Vol.29, No.12, 2011

An Investigation of Natural Convection Heat Transfer in a Square Enclosure Filled with Nanofluid

Ayad M. Salman*

Received on: 6/4/2011
Accepted on: 21/7/2011

Abstract

In this research, numerical solution of natural convection heat transfer of nanofluids in two-dimensional square enclosures is obtained for different values of Rayleigh numbers and volume fraction of nanofluids. Numerical simulation has then been undertaken for the mixture of Cu-water as nanofluid.

The stream–vorticity form of the Navier–Stokes equations and energy equation are used in this study. The present model is utilized to obtain results in the range of Rayleigh number 10^3–10^5 and volume fractions of nanofluids (0.025-0.1). The enclosure which represent two-dimensional square enclosure with heated left side wall, while the right side was cold, the top and bottom walls were adiabatic. The governing equations are solved with finite-difference technique by central difference scheme. A computer program in (FORTRAN 90) was used to carry out the numerical solution.

The results are a remarkable increase in the average Nusselt number with an increase in the volume fraction. An increase in the Rayleigh number results an increase in the average Nusselt number for a certain nanoparticle.

In order to validate the numerical model, the results of two previous works for square enclosure filled by water based Al_2O_3 nano-particles as nanofluids. The first work was variation of average Nusselt number and volume fraction for Ra number $Ra=10^3$. There are excellent agreement in results and the maximum difference between these results reach 4.2%. A relation between average Nusselt number and Ra number also compared for other previous work. There are agreement in results and found the maximum difference between results reach to 6.5% approximately at $Ra=10^5$ which validate the present computational model.

Keywords: natural convection, nanofluid, stream-vorticity form, finite difference, square enclosure.

تنبؤ انتقال الحرارة بالحمل الحر في حيز مربع مملؤ بمائع متناهي الصغر (مائع نانوي)

الخلاصة

في هذا البحث تم الحصول على الحل العددي لانتقال الحرارة بالحمل الحر للموائع المتناهية الصغر (الموائع النانوية) في حيز مربع مغلق ثنائي الابعاد لقيم مختلفة من ارقام رالي والنسب الحجمية للمائع المتناهي الصغر (المائع النانوي). المحاكة العددية تم انجازها او تنفيذها لخليط من الماء والنحاس كمائع نانوي. استخدمت صياغة الدوامية ودالة الانسياب لمعادلات (Navier–Stokes) ومعادلة الطاقة في الدراسة النظرية. النموذج الحالي استخدم للحصول على النتائج لهدى ارقام رالي (10^3–10^5) ونسب حجمية للمائع النانوي (0.025-0.1). الحيز المربع المستخدم هو ثنائي الأبعاد مع تسخين الجانب الأيسر من الحيز، في حين أن الجانب الأيمن باردا، اما الجدران العلوية والسفلية معزولة. المعادلات الحاكمة تم حلها بتقنية الفروق المحددة بواسطة اسلوب الفروقات المركزية. تم بناء برنامج حاسوبي بلغة (فورتران 90) لتنفيذ الحل العددي. النتائج تشير الى زيادة معدل رقم نسلت مع زيادة النسب الحجمية وزيادة ارقام رالي. لتأكيد النتائج العددية فقد تم مقارنتها مع نتائج عملين سابقين لحيز مربع مملؤ الماء وجزيئات Al_2O_3 النانوية كمائع نانوي.

***Energy and Fuel Research Center, University of Technology /Baghdad**

https://doi.org/10.30684/ etj.29.12.1
University of Technology-Iraq, Baghdad, Iraq/2412-0758

العمل الأول كان لتغير معدل رقم نسلت مع النسب الحجمية لرقم رالي 10^3 وكان هناك توافق بين النتائج وأقصى فرق في النتائج يصل إلى 4.2%. أيضا تم مقارنة العلاقة بين معدل رقم نسلت ورقم رالي مع عمل سابق اخر وكان هناك توافق بين النتائج وأقصى فرق في النتائج يصل إلى 6.5% تقريبا. مما يؤكد موثوقية النموذج الحسابي الحالي.

Nomenclature

The following symbols are used generally throughout the text. Others are defined as and when used.

Symbols	Meaning	Units
C_p	Specific heat at constant pressure	J/kg.K
E_{max}	Maximum error	——
g	Gravitational acceleration	m/s^2
k	Thermal conductivity	W/m.K
L	Side of the square cavity	m
Nu	Nussel number	——
$\overline{Nu}$	Average Nussel number	——
P	Pressure	Pa
Pr	Prandtl number	——
Ra	Rayleih number	——
$r, r_\Psi, r_\Omega, r_\theta$	Relaxation parameter for stream function, vorticity, and temperature	——
T	Temperature	K
u, v	Velocity components in x- and y- direction	m/s
U, V	Dimensionless velocity component in X- and Y-directions	
x, y	Cartesian space coordinates	m
X,Y	Dimensionless Cartesian space coordinates	——
Greek Symbol		
α	Thermal diffusivity	m^2/s
β	Coefficient of thermal expansion	1/K
ϕ	Volume fraction	——
φ	General dimensionless dependent variable (Ψ, ω, θ)	——
μ	Molecular dynamic viscosity	$N.s/m^2$
ν	Kinematic viscosity	m^2/s
ω	Vorticity	1/s
Ω	Dimensionless vorticity	——
ψ	stream function	m^2/s
Ψ	Dimensionless stream function	——
ρ	Density	kg/m^3
θ	Dimensionless temperature	——
Subscript Symbols		
C, H	Related to cold and hot side respectively	——
(i,j)	Grid nodes in (X,Y) direction	——
eff	Effective	——
f	Fluid	——
nf	Nanofluid	——
s	Solid	——

1. Introduction

Nanofluids, i.e. fluid suspensions of nanometer-sized solid particles and fibers, have been proposed as a route for surpassing the performance of heat transfer of liquids currently available. Recent experiments on nanofluids have indicated significant increases in thermal conductivity compared with liquids without nanoparticles or larger particles, strong temperature dependence of thermal conductivity, and significant increases in critical heat flux in boiling heat transfer. Some of the experimentalresults are controversial, e.g. the extent of thermal conductivity enhancement sometimes greatly exceeds the predictions of wellestablished theories. So, if these exciting results on nanofluids can be confirmed in future systematic experiments, new theoretical descriptions may be needed to account properly for the unique features of nanofluids, such as high particle mobility and large surface-to-volume ratio (Keblinski1 et al., 2005))Improvements to make heat transfer equipment more energy efficient would need to focus on miniaturization on the one hand and an astronomical increase in heat flux on the other. Heat transfer fluids such as water, mineral oil and ethylene glycol play a vital role in many industrial processes, including power generation, chemical processes, heating or cooling processes, and microelectronics. The poor heat transfer properties of these common fluids compared to most solids is a primary obstacle to the high compactness and effectiveness of

Heat exchangers. The essential initiative is to seek the solid particles

Having thermal conductivities several hundreds of times higher than

Those of conventional fluids. An innovative idea is to suspend ultra fine solid particles in the fluid for improving the thermal conductivity of a fluid. Many types of particle, such as metallic, non-metallic and polymeric, can be added into fluids to form slurries. However, the usual slurries, with suspended particles in the order of millimeters or even micrometers may cause some severe problems. The abrasive action of the particles causes the clogging of flow channels, erosion of pipelines and their momentum transfers into an increase in pressure drop in practical applications. Furthermore, they often suffer from instability and archeological problems. In particular, the particles tend to settle rapidly. Thus, although the slurries give better thermal conductivities, they are not practical.

Fluid heating and cooling are important in many industries such as power, manufacturing, transportation, and electronics. Effective cooling techniques are greatly needed for cooling any sort of high-energy device. Common heat transfer fluids such as water, ethylene glycol, and engine oil have limited heat transfer capabilities due to their low heat transfer properties. In contrast, metals have thermal conductivities up to three times higher than these fluids, so it is natural that it would be desired to combine the two substances to produce a heat transfer medium that behaves like a fluid, but has the thermal conductivity of a metal. Nanofluids are made of nanoparticles suspended in a base fluid. Typical nanoparticles are metal or metal oxide nanoparticles such as Al_2O_3, CuO, Cu,

TiO. Generally water and ethylene glycol is used as the base fluid (Kakac and Pramuanjaroenkij, 2009).

Because of the practical importance of natural convection heat transfer in an enclosure filled by nanofluids, this research presents numerical study for natural convection in square enclosure filled by nanofluids, through the following research plan:

i. Mathematical modeling of the problem including the governing equations (conservation and constitution laws) with the proper boundary conditions. After that these equations will be converted to dimensionless form then the stream function and vorticity (Ψ-Ω) scheme will be applied on these equations and it will be solved numerically by finite difference technique.
ii. Make computational model to solve the derived mathematical model numerically. Central finite Difference scheme will be used in the numerical formulation.
iii. A computer program will be built to perform the numerical calculation algorithm developed in (ii) above.
iv. Parametric study will be made by using the computer program to investigate the effect of various thermal parameters on the performance of the problem for for several values of Rayleigh number (Ra) from (10^3-10^5) and nanoparticle volume fraction of nanoparticle (ϕ) for Cu based nanofluids which ranging within (0.025-0.1).
v. Verification of the developed computational algorithm through a comparison with previous available works and analysis and discussion of the results for final.

The previous related literatures dealt with the subject of the research will be presented.

Khanafer et al. (2003) developed an analytical model to determine natural convective heat transfer in nanofluids. The nanofluid in the enclosure was assumed to be a single phase. The effect of suspended nanoparticles on a buoyancy-driven heat transfer process was analyzed. It was observed that the heat transfer rate increased as the particle volume fraction increased at any given Grashof number.

Hwang et al. (2007) investigated theoretically of thermal characteristics of natural convection in a rectangular cavity heated from below with water-based nanofluids containing alumina (Al_2O_3 nanofluids). The ratio of heat transfer coefficient of nanofluids to that of base fluid is decreased as the size of nanoparticles increases, or the average temperature of nanofluids is decreased.

Abu-Nada et al. (2008) studied numerically of heat transfer enhancement in horizontal annuli using nanofluids is investigated. Water-based nanofluids containing various volume fractions of Cu, Ag, Al_2O_3 and TiO_2 nanoparticles is used. For $Ra=10^3$ and $Ra=10^5$ the addition of Al_2O_3 nanoparticles improves heat transfer. And, for $Ra=10^4$, the addition of nanoparticles has a very minor effect on heat transfer characteristics.

Oztop and Abu-Nada (2008) studied numerically heat transfer and fluid flow due to buoyancy forces in a partially heated enclosure using nanofluids is carried out using different types of nanoparticles, The finite volume technique is used to solve the governing equations. Calculations were performed for Rayleigh number ($10^3 \leq Ra \leq 10^5$) and height of heater within ranging (0.1-0.75). An increase in mean Nusselt number was found with the volume fraction of nanoparticles for the whole range of Rayleigh number. Heat transfer also increases with increasing of height of heater.

Abu-Nada and Oztop (2009) studied effects of inclination angle on natural convection heat transfer and fluid flow in a two-dimensional enclosure filled by nanofluids has been analyzed numerically. The governing equations are solved with finite-volume technique for the range of Rayleigh numbers as $10^3 \leq Ra \leq 10^5$. The effect of nanoparticles concentration on Nusselt number is more pronounced at low volume fraction than at high volume fraction. Inclination angle can be a control parameter for nanofluid filled enclosure.

Anilkumar and Jilani (2009) studied numerically of two-dimensional enclosure for a range of Rayleigh numbers (10^3-10^4), fin heights and aspect ratios. The flow and temperature distributions are taken to be two-dimensional. Regions with the same velocity and temperature distributions are identified as symmetry of sections. As Rayleigh number increases natural convection prevails, the temperature variation is restricted over a gradually diminishing region around the fin. It is also noticed that the heat affected zone becomes larger with the increasing fin height.

Li and Peterson (2009) Studied experimentally the natural convection heat transfer characteristics of Al_2O_3/water nanofluids comprised of 47 nm, Al_2O_3 and water, with volume fractions ranging from 0.5% through 6%, has been investigated through a set of experimental measurements. The influence of particle movements on the heat transfer and natural flow of the polystyrene particle/DI water suspension were filmed, and the temperature changes on the heating and cooling surfaces were recorded.

Sapna and Gupta (2009) the heat transfer and fluid flow due to buoyancy force in a square enclosure using nanofluids are studied. Four different types of model from the literature are considered for the effective viscosity of the nanofluids. Simulations have been carried out to investigate the effects of the volume fraction, Nusselt number and Grashof number. An increase in Nusselt number was found with the volume fraction of nanoparticles for the whole range of Grashof number.

Lin and Violi (2010) analyzed the heat transfer and fluid flow of natural convection in a cavity filled with Al_2O_3 water nanofluids that operates under differentially heated walls. The increase of nanofluid temperature is found to augment both the effects of non-uniform nanoparticle diameter and mean nanoparticle diameter inside the cavity.

Shahi et al. (2010) made 3D numerical simulation for steady natural convective flow and heat transfers a single-ended tube with non-uniform heat input. The governing equations have been then approximated by means of a fully

implicit finite volume method (FVM), using SIMPLE algorithm on the collocated arrangement. The study has been carried out for solid volume fraction $0 \le \phi \le 0.05$ and maximum heat flux $100 \le q'' \le 700$. The effect of the inclination angle indicated that the maximum overall mean Nusselt number is obtained at 35°, while the maximum output mass flow rate is increasing function of the inclination angle. It also obtained that both the Nusselt number and maximum output mass flow rate are increasing function of solid concentration, but the presence of nanoparticles is more effective at the smaller inclination angles.

Sivasankaran et al. (2010) presented numerical steady to investigat the convection flow and heat transfer of nanofluids with different nano-particles in square cavity. It was found that heat transfer rate increase on increasing the volume fraction. The increament in average Nusselt number is strongly depent on the nanoparticle chosen.

Waheed et al. (2011) studied numerically the heat function as a visualization tool used to study the heat flow in rectangular enclosures filled with nanofluids. The results show a strong effect of the volume fraction of the nanoparticles on the flow, temperature and heat function fields.

2. Mathematical Model

A schematic representation of the system under investigation is shown in figure (1), where L is side of the square enclosure cavity which is calculated depending on the Rayleigh number.

3.1 Governing Equations

The continuity, momentum and energy equations for a two dimensional incompressible laminar flow has been solved using appropriate boundary conditions by mean computational fluid dynamics technique. Following assumptions have been made: two-dimensional problem, there is no viscous dissipation, the gravity acts in the vertical direction, the fluid properties are constant and radiation heat exchange was assumed negligible. At steady state conditions using above assumption, the governing equations as given below (Ho et al., 2008):

Continuity equation:

$$\frac{\partial u}{\partial x}+\frac{\partial v}{\partial y}=0 \qquad (1)$$

x-momentum equation:

$$u\frac{\partial u}{\partial x}+v\frac{\partial u}{\partial y}=-\frac{1}{\rho_{nf}}\frac{\partial p}{\partial x}+\frac{\mu_{eff}}{\rho_{nf}}\left(\frac{\partial^2 u}{\partial x^2}+\frac{\partial^2 u}{\partial y^2}\right) \qquad (2)$$

y-momentum equation:

$$u\frac{\partial v}{\partial x}+v\frac{\partial v}{\partial y}=-\frac{1}{\rho_{nf}}\frac{\partial p}{\partial y}+\frac{\mu_{eff}}{\rho_{nf}}\left(\frac{\partial^2 v}{\partial x^2}+\frac{\partial^2 v}{\partial y^2}\right)+\frac{1}{\rho_{nf}}\left[\phi\rho_s\beta_s+(1-\phi)\rho_f\beta_f\right]g(T-T_C) \qquad (3)$$

Energy equation

$$u\frac{\partial T}{\partial x}+v\frac{\partial T}{\partial y}=\alpha_{nf}\left(\frac{\partial^2 T}{\partial x^2}+\frac{\partial^2 T}{\partial y^2}\right) \qquad (4)$$

Where g is the gravitational acceleration (m/sec^2), β is coefficient of thermal expansion. The governing equations given above, i.e., equation (1) to equation (4), are given in terms of the so-called primitive variables, i.e., u, v, p, an T. The solution procedure discussed here is

based on equations involving the stream function, the vorticity, and the temperature, as variables. The stream function and vorticity are defined by:

$$u = \frac{\partial \psi}{\partial y}, \mathrm{v} = -\frac{\partial \psi}{\partial \mathrm{x}} \quad (5)$$

$$\omega = \left(\frac{\partial \mathrm{v}}{\partial x} - \frac{\partial u}{\partial y} \right) \quad (6)$$

The vorticity equation is obtained by eliminating the pressure between the two momentum equations, i.e., by taking the y-derivative of equation (2) and subtracting from it the x-derivative of equation (3). The equation of vorticity (conservation of angular momentum) becomes

$$\frac{\partial \psi}{\partial y}\frac{\partial \omega}{\partial x} - \frac{\partial \psi}{\partial x}\frac{\partial \omega}{\partial y} = \frac{\mu_{nf}}{\rho_{nf}}\left(\frac{\partial^2 \omega}{\partial x^2} + \frac{\partial^2 \omega}{\partial y^2} \right) + \frac{1}{\rho_{nf}}\left[\phi \rho_s \beta_s + (1-\phi)\rho_f \beta_f \right] g \frac{\partial T}{\partial x} \quad (7)$$

In terms of stream function, the equation become

$$\left(\frac{\partial^2 \psi}{\partial x^2} + \frac{\partial^2 \psi}{\partial y^2} \right) = -\omega \quad (8)$$

While in terms of the stream function the energy equation becomes

$$\frac{\partial \psi}{\partial y}\frac{\partial T}{\partial x} - \frac{\partial \psi}{\partial x}\frac{\partial T}{\partial y} = \alpha_{nf}\left(\frac{\partial^2 T}{\partial x^2} + \frac{\partial^2 T}{\partial y^2} \right) \quad (9)$$

The effective physical properties of the nanofluids in the above equations are:

The viscosity of the nanofluids can be approximated as viscosity of a base fluid μ_f is given by **(**Brinkman, 1952 and Ho et al. 2008**)**

$$\mu_{nf} = \frac{\mu_f}{(1-\phi)^{2.5}} \quad (10)$$

The density of the nanofluid is given as

$$\rho_{nf} = (1-\phi)\rho_f + \phi \rho_s \quad (11)$$

The thermal diffusivity of the nanofluid is given as

$$\alpha_{nf} = \frac{k_{nf}}{(\rho C_p)_{nf}} \quad (12)$$

The heat capacity of the nanofluid is expressed as (Abu-Nadu, 2008 and Khanafer et al. 2003)

$$(\rho C_p)_{nf} = (1-\phi)(\rho C_p)_f + \phi (\rho C_p)_s \quad (13)$$

The thermal conductivity of nanofluid is approximated as (Abu-Nadu, 2008 and Khanafer et al. 2003)

$$k_{nf} = k_f \frac{(k_s + 2k_f - 2\phi(k_f - k_s))}{(k_s + 2k_f + \phi(k_f - k_s))} \quad (14)$$

Before considering the numerical solution to the above set of equations, it is convenient to rewrite the equations in terms of dimensionless variables. The following dimensionless variables will be used here (Oosthuizen and Naylor, 1999):

$$\left.\begin{aligned} &\Psi = \frac{\psi}{\alpha_f}, \Omega = \frac{\omega \mathrm{L}^2}{\alpha_f} \\ &X = \frac{x}{L}, \mathrm{Y} = \frac{\mathrm{y}}{\mathrm{L}} \\ &\theta = \frac{T - T_c}{T_h - T_c} \\ &Ra = \frac{g\beta(T_H - T_C)L^3}{\nu^2}, \ \mathrm{Pr} = \frac{\nu}{\alpha} \end{aligned}\right\} \quad (15)$$

terms of these variables, the stream function, vorticity and energy equations respectively becomes

$$\left(\frac{\partial^2 \Psi}{\partial X^2} + \frac{\partial^2 \Psi}{\partial Y^2} \right) = -\Omega \quad (16)$$

$$\frac{\partial \Psi}{\partial Y}\frac{\partial \Omega}{\partial X}-\frac{\partial \Psi}{\partial X}\frac{\partial \Omega}{\partial Y}= a_1\left(\frac{\partial^2 \Omega}{\partial X^2}+\frac{\partial^2 \Omega}{\partial Y^2}\right)+a_2\frac{\partial \theta}{\partial X} \qquad (17)$$

Where

$$a_1=\mathrm{Pr}\Big/\left[(1-\phi)^{0.25}\left((1-\phi)+\phi\frac{\rho_s}{\rho_f}\right)\right]$$

$$a_2=Ra\,\mathrm{Pr}\Big/\left[\frac{1}{\frac{(1-\phi)\rho_f}{\phi\rho_s}+1}\frac{\beta_s}{\beta_f}+\frac{1}{\frac{\phi\rho_f}{(1-\phi)\rho_s}+1}\right]$$

$$\frac{\partial \Psi}{\partial Y}\frac{\partial \theta}{\partial X}-\frac{\partial \Psi}{\partial X}\frac{\partial \theta}{\partial Y}=\lambda\left(\frac{\partial^2 \theta}{\partial X^2}+\frac{\partial^2 \theta}{\partial Y^2}\right) \qquad (18)$$

Where

$$\lambda=\frac{k_{nf}/k_f}{(1-\phi)+\phi\frac{(\rho C_p)_s}{(\rho C_p)_f}}$$

3.2 Boundary Conditions

The boundary conditions of velocity and temperature fields are shown in figure (1) presented as (Oosthuizen and Naylor (1999)):

$$\left.\begin{aligned} &X=0: u=v=\Psi=0,\ \theta=1,\ \Omega=-\frac{\partial^2\Psi}{\partial X^2}\\ &X=1:\ u=v=\Psi=0,\ \theta=0,\ \Omega=-\frac{\partial^2\Psi}{\partial X^2}\\ &Y=0: u=v=\Psi=0,\ \frac{\partial\theta}{\partial Y}=0,\ \Omega=-\frac{\partial^2\Psi}{\partial Y^2}\\ &Y=1: Y=0: u=v=\Psi=0,\ \frac{\partial\theta}{\partial Y}=0,\ \Omega=-\frac{\partial^2\Psi}{\partial Y^2}\end{aligned}\right\} (19)$$

The boundary conditions of velocity and temperature fields are shown in figure (1) can be expressed in table (1).

4. Numerical Solution

An iterative finite difference solution procedure will be used. The method of numerical solution taken is the central finite difference scheme technique for convert the partial differential equation to an algebraic which can be solved numerically. The energy equation is a nonlinear partial differential equation, which has (convection terms) on the left hand side of the equation (18) and (diffusion term) on the right hand side. To convert the convection and diffusion terms to algebraic terms, central difference scheme will be used, as below and can be rearranged to give (Tannehill et al. (1997))

$$\theta_{i,j}=\left\{\left(\frac{-1}{4\Delta X\Delta Y}\frac{1}{\lambda}\right)\left[\begin{aligned}&\left(\Psi_{i,j+1}-\Psi_{i,j-1}\right)\left(\theta_{i+1,j}-\theta_{i-1,j}\right)-\\&\left(\Psi_{i+1,j}-\Psi_{i+1,j}\right)\left(\theta_{i,j+1}-\theta_{i,j-1}\right)\end{aligned}\right]+\left(\frac{\theta_{i+1,j}+\theta_{i-1,j}}{\Delta X^2}+\frac{\theta_{i,j+1}+\theta_{i,j-1}}{\Delta Y^2}\right)\right\}\Bigg/\left(\frac{2}{\Delta X^2}+\frac{2}{\Delta Y^2}\right) \qquad (20)$$

Similarity, the finite difference form of the vorticity transport equation, i.e., equation (17), gives

$$\Omega_{i,j}=\left\{\left(\frac{-1}{4\Delta X\Delta Y}\frac{1}{a_1}\right)\left[\begin{aligned}&\left(\Psi_{i,j+1}-\Psi_{i,j-1}\right)\left(\Omega_{i+1,j}-\Omega_{i-1,j}\right)-\\&\left(\Psi_{i+1,j}-\Psi_{i+1,j}\right)\left(\Omega_{i,j+1}-\Omega_{i,j-1}\right)\end{aligned}\right]+\left(\frac{\Omega_{i+1,j}+\Omega_{i-1,j}}{\Delta X^2}+\frac{\Omega_{i,j+1}+\Omega_{i,j-1}}{\Delta Y^2}\right)-\frac{a_2}{a_1}\left(\frac{\theta_{i+1,j}-\theta_{i-1,j}}{2\Delta X}\right)\right\}\Bigg/\left(\frac{2}{\Delta X^2}+\frac{2}{\Delta Y^2}\right) \qquad (21)$$

Lastly, the finite difference form of the equation relating the

dimensionless stream function, i.e., equation (16), is

$$\Psi_{i,j}=\left[\left(\frac{\Psi_{i+1,j}+\Psi_{i-1,j}}{\Delta X^2}+\frac{\Psi_{i,j+1}+\Psi_{i,j-1}}{\Delta Y^2}\right)+\Omega_{i,j}\right]\Big/\left(\frac{2}{\Delta X^2}+\frac{2}{\Delta Y^2}\right) \quad (22)$$

4.2 Nusselt Number Calculations

The local heat transfer rate along the heated wall is obtained from the heat balance that gives an expression for local Nusselt number as (Lin and Violi, 2010)

$$Nu=-\frac{k_{nf}}{k_f}\frac{\partial\theta}{\partial X}\bigg|_{X=0} \quad ; \quad 0\le Y\le 1 \quad (23)$$

In difference form this can be written as

$$Nu=\frac{k_{nf}}{k_f}\left(\frac{25\theta_{1,j}-48\theta_{2,j}+36\theta_{3,j}-16\theta_{4,j}+3\theta_{5,j}}{12\Delta X}\right) \quad (24)$$

The average value for Nusselt number is defined by

$$\overline{Nu}=\frac{1}{L}\int_0^L NudX \quad (25)$$

This equation can be readily evaluated using Simpson's rule.

4.3 Solution Procedure

The governing dimensionless differential equations are discretized to a finite difference form, central difference scheme is used. The iterative routine, the selected grid and the relaxation parameters are verified at different Rayleigh numbers. The computational scheme, based on Successive Relaxation, SR, is arranged to solve the three equations for the n th iteration step. The initial values over the field for θ, ω and ψ are assumed zero to all internal nodes are taken as initial starting values. Relaxation is actually used so the "updated" values of $\varphi_{i,j}$ are actually taken as:

$$\varphi_{i,j}^{new}=\varphi_{i,j}^{old}+r\left(\varphi_{i,j}^{calculated}-\varphi_{i,j}^{old}\right) \quad (26)$$

Where the subscripts i and j refer to a grid node, φ is a general dependent variable (θ, ω, or ψ). The relaxation parameters, $r_\theta = r_\omega = 1$ and $r_\psi = 1.6$ give stable numerical computation, for higher Ra values $r_\theta = 1$, $r_\omega = 0.1$ to .02 and r_ψ=1.97 are used.

The criterion for convergence is examined according to a realistic condition for each state variable at each node as:

$$\frac{\left|\varphi_{i,j}^{new}-\varphi_{i,j}^{old}\right|}{\left|\varphi_{i,j}^{old}\right|}\le \text{Emax} \quad (27)$$

Where the subscripts i and j refer to a grid node, φ is a general dependent variable (θ, ω, or ψ) and E_{max} is a small quantity of error set to 10^{-5} for $Ra \le 10^4$ and set to 10^{-4} for $Ra \ge 10^5$. the grid size of enclosure is 47×47 for $Ra \le 10^4$ and finer uniform grid (67×67) for $Ra=10^5$ are used to improve the results at $Ra=10^5$.

A computer program in (Fortran 90) was built to execute the numerical algorithm which is mentioned above; it is general for a natural convection in two-dimensional enclosure filled by nanofluid.

5. Results and Discussion

The numerical results are reported for several values of Rayleigh number (Ra) from 10^3 to 10^5 and nanoparticle volume fraction (ϕ) for copper (Cu) based nanofluids which ranging within (0.025 to 0.1). The Prandtl number (Pr) is 6.2 which mean the base fluid is water. The results obtained are discussed under different

combinations of pertinent parameters involved in the study.

Figure (2) illustrates the effect of Ra number on the steady-state variation of the streamlines, vorticity and isotherms contours for Ra $=10^3$-10^5 and ϕ= 0.025. The intensity of flow activities is documented by recording the values of streamline contours. In this physical model, the flow patterns are characterized by a primary recirculating clockwise vortex that occupies the bulk of the cavity. As Ra number increases from 10^3 to 10^5, the flow patterns remain quite the same while the absolute circulation strength is enhanced due to relatively high velocity of the fluid flow.

By looking at the sign of the gradient for the stream function in the x-direction, we can find that the vortices are rotating in the clockwise direction. The vortex moves the warm fluid from the left wall along the top of the geometry and results in higher temperatures at the top half of cavity.

When the nanofluids be colder it becomes heavy and its density increased so it moves downward and it will be circulate again towards the hot wall and this will be repeated until a balance of temperature distribution will be reached in square enclosure. Also showed streamlines for ($Ra=10^3$,10^4) will be almost similar except that in $Ra=10^5$, the streamlines will be closer to the wall, this mean means that the buoyancy force increase causes an accelerate flow.

Vorticity lines ($Ra=10^3$,10^4), they showed multi-cellular flow regime appears. This effect is more pronounced at high Rayleigh numbers where multicellular flow patterns dominate. The strength of the vortices is also increased as seen by the magnitude of the stream function gradient.

Isotherms contours for ranging ($Ra=10^3$,10^4 and 10^5). From this figure the heat transfer operation can be divided into multi region, first region is that of heat transfer by conduction which extended to ($Ra\leq10^3$). The second region is transition region until plum region is appeared and ranged (10^3 <Ra $\leq10^4$). Third region is the plume region which is at ($Ra>10^4$), so when Ra increase plume region will be more clear especially at ($Ra=10^5$). The parallel isothermal lines away from the heated wall at low Rayleigh number, $Ra=10^3$, indicate conduction dominated mode of heat transfer, though convection is developed in the layer adjacent to the heated wall.

Figures (3), (4) and (5) show the effect of volume fraction for different Rayleigh numbers on Cu based nanofluids. When volume fraction increases from 0.05 to 0.1 flow strength increases. More fluid is heated. This behaviour can be seen from the isotherms. Also shows isotherms for ranging ($Ra=10^3$,10^4). From these figures the heat transfer operation can be divided into multi region, first region is transition region until plum region is appeared and ranged (10^3 $\leq$Ra $\leq10^4$). The second region is the plume region which is at ($Ra\geq10^4$), so when Ra increase plume region will be more clear especially at ($Ra=10^5$). This analysis basically implies that at a constant volume fraction, the heat convection is better enhanced with increase volume fraction, with these nanoparticle structures, the value of dimensionless thermal conductivity k_{nf}/k_f increases.

The comparisons of the pure fluid and nanofluid isotherms show that vertical stratification of the isotherms breaks down with an increase in volume fraction at relatively high Ra number. It is clear from these figures that the heat transfer increase when increasing the volume fraction of nanoparticles. Generally, for low Ra the streamlines and isotherms are

uniform due to quasi-conduction heat transfer regime where formed clearly, but if Ra increase the convection heat transfer region become clear streamlines and isotherms become non uniform and random.

The Nusselt number is an important non-dimensional parameter in convective heat transfer. Thus, the Nusselt number for several volume fraction of nanofluids at different Rayleigh number is briefly sketched in Figures (6), (7) and (8) respectively. It is interesting to indicate that the maximum values of the Nusselt number along the y direction is not at bottom wall, but close to the bottom wall. An initial look at the range of the Nusselt number values shown in these figures clearly indicates that the Nusselt number increases with increase in the value of the Rayleigh number and volume fraction as expected. When convective heat transport reaches minimum at lower value of Rayleigh number and volume fraction, the value of the Nusselt number is smaller compared to higher Rayleigh number volume fraction of nanofluids. The pronounced convective heat transfer due to the increase in value of the Rayleigh number to 10^5 is vividly indicated in Figure (8).

Figure (9) shows the variation of average Nusselt number with respect to volume fraction, Rayleigh number copper-water based nanofluids. There is a remarkable increase in the average Nusselt number with an increase in the volume fraction. An increase in the Rayleigh number results an increase in the average Nusselt number for a certain nanoparticle.

In order to validate the numerical model, a relation between average Nusselt number and volume fraction at $Ra=10^3$ in figure (10) is compared with numerical results of ref. [6]. The best agreement at $\phi=0.1$ and the maximum difference between these results reach to 4.2%. Figure (11) shows a comparison between average Nusselt number of Al_2O_3 nanofluid for volume fraction $\phi=0.04$ with results ref. [13]. It is clearly seen from this figure that there is best agreement between the results at $Ra=10^3$ and 10^4 and the difference reach to 6.5% approximately at $Ra=10^5$.

6. Conclusions

A numerical study has been performed to investigate the effect of using different nanofluid on natural convection flow field and temperature distribution in heated square enclosure from left vertical wall. Some important points can be drawn from the obtained results such as

a) Flow strength and heat transfer are increasing generally in nano-fluid case comparing with pure fluid case.
b) Increasing the value of Rayleigh number enhance the heat transfer and flow strength keeping other parameters fixed.
c) Heat transfer is increased with increasing the value of volume fraction of nanoparticales.
d) The variation of average Nusselt number with respect to volume fraction, Rayleigh number copper-water based nanofluid. There is a remarkable increase in the average Nusselt number with an increase in the volume fraction. An increase in the Rayleigh number results an increase in the average Nusselt number for a certain nanoparticle.

References

[1] Keblinski1, Pawel, Eastman, Jeffrey A. and Cahill, David G., 2005, "Nanofluids for thermal transport", Elsevier Ltd.

[2] Kakac S., Pramuanjaroenkij, A., Review of convective heat transfer enhancement with nanofluids, Int. J. of Heat and Mass Transfer, Vol. 52, pp.(3187-3196).

[3] Khanafer, Khalil, Vafai, Kambiz, and Lightstone, Marilyn, 2003, "Buoyancy-driven heat transfer enhancement in a two-dimensional enclosure utilizing nanofluids", Int. J. Heat and Mass Transfer, Vol. (46), pp. (3639–3653).

[4] Hwang, Kyo Sik, Lee, Ji-Hwan, Jang, Seok Pil Jang, 2007, "Buoyancy-driven heat transfer of water-based Al_2O_3 nanofluids in a rectangular cavity", Int. J. Heat and Mass Transfer, Vol. (50), pp. (4003–4010).

[5] Abu-Nada, E., Masoud Z., Hijazi, A., 2008, "Natural convection heat transfer enhancement in horizontal concentric annuli using nanofluids", Int. Communications J. Heat and Mass Transfer, Vol. 35, pp.(657–665).

[6] Oztop, Hakan F. and Abu-Nada, Eiyad, 2008, "Numerical study of natural convection in partially heated rectangular enclosures filled with nanofluids", Int. J. Heat and Fluid Flow, Vol. (29), pp. (1326–1336).

[7] Abu-Nada, Eiyad and Oztop, Hakan F., 2009, "Effects of inclination angle on natural convection in enclosures filled with Cu–water nanofluid" Int. J. Heat and Fluid Flow, pp. (1-10).

[8] Anilkumar, S.H. and Jilani, G., (2009), "Convective Heat Transfer Enhancement in an Enclosure with Fin utilizing Nanofluids", International Journal of Aerospace and Mechanical Engineering, Vol. 3, No. 2, pp. (104-111).

[9] Li, Calvin H. and Peterson, G. P., (2009), "Experimental Studies of Natural Convection Heat Transfer of Al2O3/DIWater Nanoparticle Suspensions (Nanofluids)', Advances in Mechanical Engineering, Volume 2010, pp. (1-10), Hindawi Publishing Corporation.

[10] Sapna Sharma, Arvind Kumar Gupta, (2009), "Numerical Simulation of Heat Transfer of Nanofluids in an Enclosure", Seventh International Conference on CFD in the Minerals and Process Industries
CSIRO, Melbourne, Australia.

[11] Lin, Kuang C. and Violi, Angela, (2010), "Natural convection heat transfer of nanofluids in a vertical cavity: Effects of non-uniform particle diameter and temperature on thermal conductivity", Int. J. Heat and Fluid Flow, Vol. 31, pp. (236–245).

[12] Shahi, Mina , Mahmoudi, Amir Houshang and Talebi, Farhad, (2010), "Numerical simulation of steady natural convection heat transfer in a 3-dimensional single-ended tube subjected to a nanofluid", Int. Com. Heat and Mass Transfer, Vol. (37), pp. (1535–1545).

[13] Sivasankaran, Sivanandam, Aasaithambi, Thangaraj and Rajan, Subbarayagounder, 2010, " Natural Convection of Nanofluids in a Cavity with Linearly Varying Wall Temperature", Maejo Int. J. Science and Technology, Vol. 4, No. 3, pp.(468-482).

[14] Waheed, M. A., Odewole, G.A., S.O., Alagbe, Kuye, S. I. and Ismaila, S. O., 2011, "Visualization of Buoyancy Induced Heat Flow in Rectangular Enclosures Filled with Nanofluids Using Heatfunction Formulation Approach", Second African Conference on Computational Mechanics– An International Conference – AfriCOMP11, January 5 – 8, Cape Town.

[15] Ho, C. J., Chen, M. W. and Li, Z. W., 2008, "Numerical simulation of natural convection of nanofluid in a square enclosure: Effects due to uncertainties of viscosity and thermal conductivity", Int. J. Heat Mass Transf., Vol. 51, pp. (4506-4516).

[16] Brinkman, H. C., 1952, "The viscosity of concentrated suspensions and solution", J. Chem. Phys., Vol. 20, pp. (571-581).

[17] Abu-Nada, E., 2008. Application of nanofluids for heat transfer enhancement of separated flows encountered in a backward facing step. Int. J. Heat Fluid Flow, Vol. 29, pp. (242–249).

[18] Oosthuzen, Patrirck H. and Naylor, David, (1999), "An Introduction to Convective Heat Transfer Analysis", International Edition, WCB/McGraw Hill, New York.

[19] Tannehill, John C., Anderson, Dale A., Pletcher, Richard H., 1997, "Computation fluid mechanics and heat transfer", 2nd Edition, Taylor & Francis, USA.

Table (1): illustrated boundary conditions of problem.

X	Y	θ	$\frac{\partial \theta}{\partial X}$	(U, V, ψ)	ω
0	Y	1	-	0	$-\frac{\partial^2 \psi}{\partial X^2}$
1	Y	0	-	0	$-\frac{\partial^2 \psi}{\partial X^2}$
X	0	-	0	0	$-\frac{\partial^2 \psi}{\partial Y^2}$
X	1	-	0	0	$-\frac{\partial^2 \psi}{\partial Y^2}$

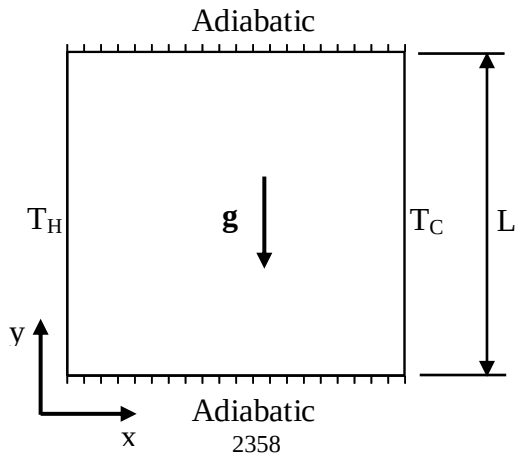

Figure (1): schematic diagram of the physical system.

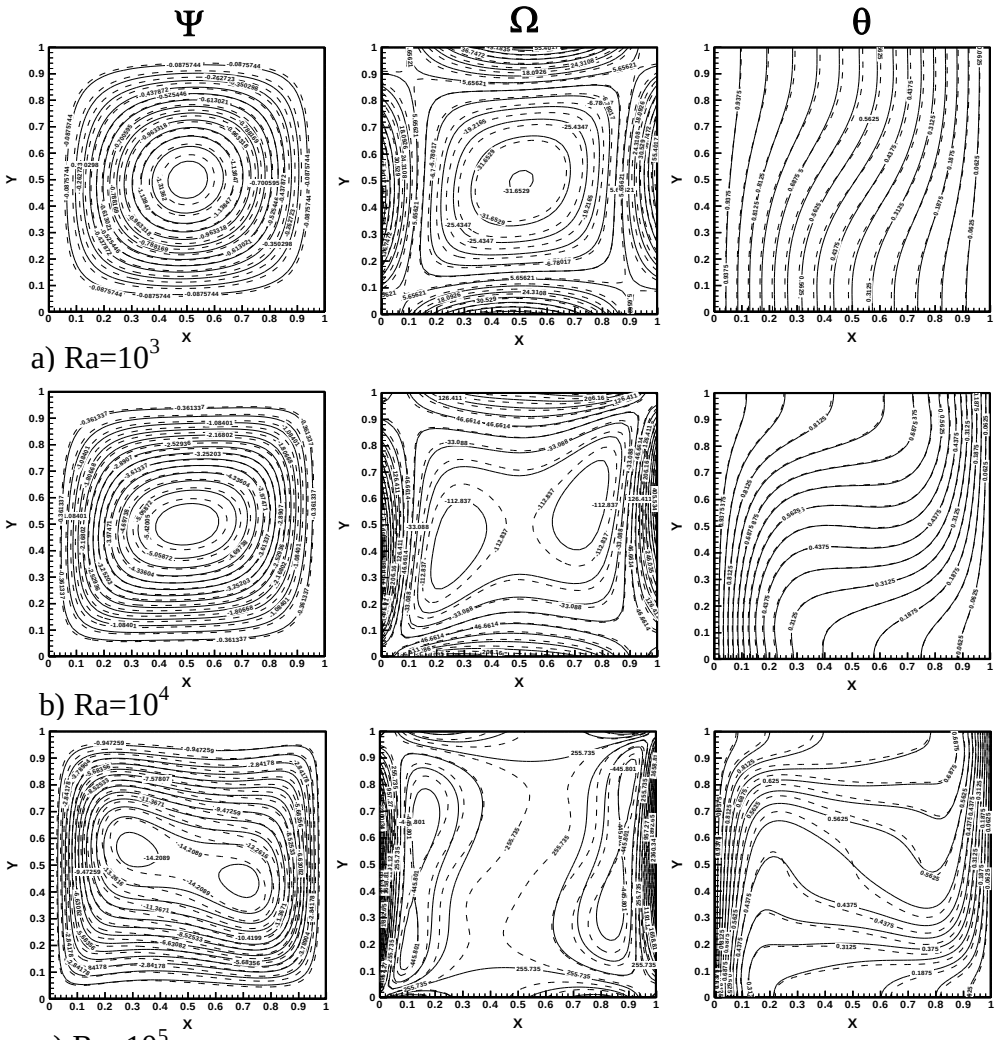

a) Ra=10^3

b) Ra=10^4

c) Ra=10^5

Figure (2): streamlines, vorticity lines and isotherms contours for pure fluid (solid lines) and nanofluids (dash lines) (ϕ=0.025) at different Rayleigh numbers.

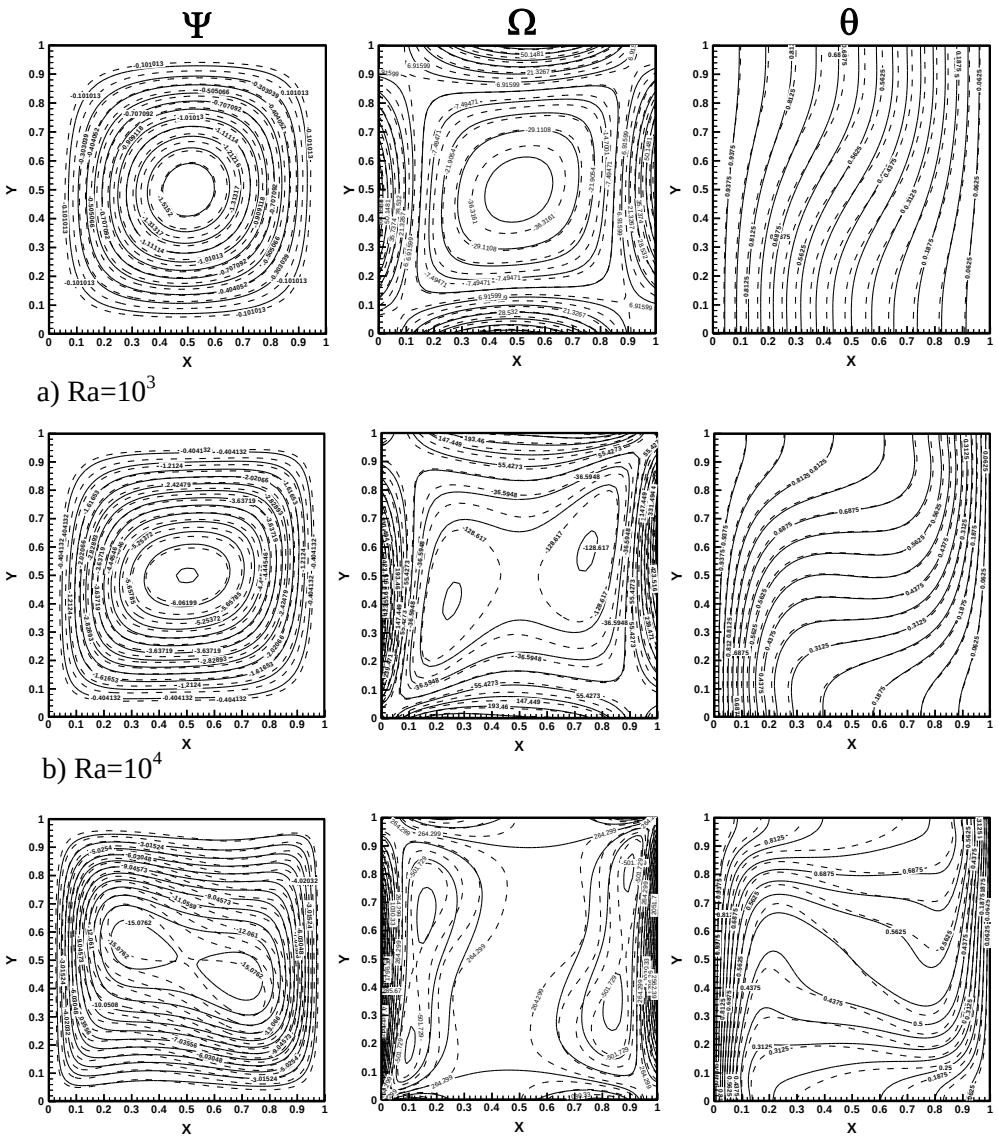

a) Ra=10^3

b) Ra=10^4

c) Ra=10^5

Figure (3): streamlines, vorticity lines and isotherms contours for pure fluid (solid lines) and nanofluids (dash lines) (ϕ=0.05) at different Rayleigh numbers.

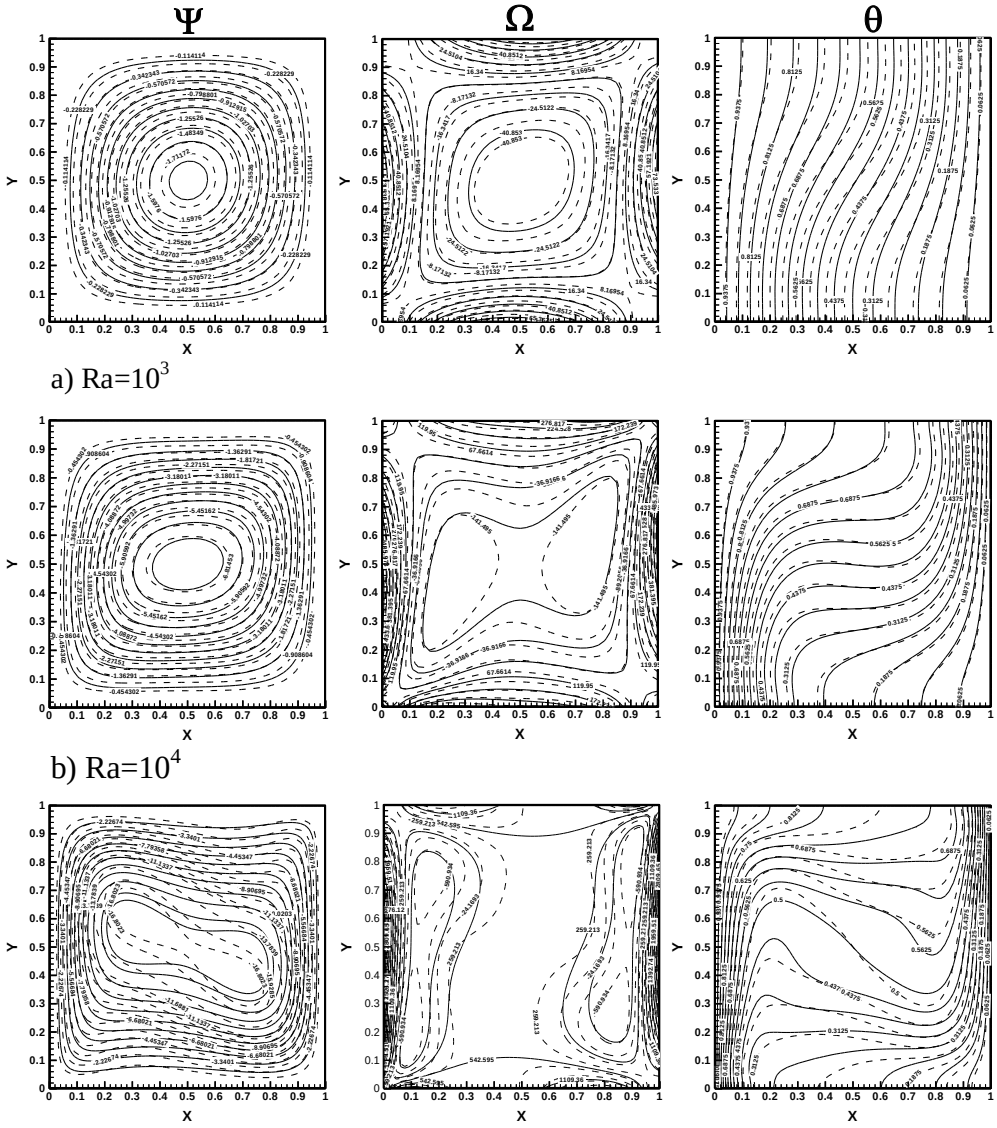

a) Ra=10^3

b) Ra=10^4

c) Ra=10^5

Figure (4): streamlines, vorticity lines and isotherms contours for pure fluid (solid lines) and nanofluids (dash lines) (ϕ=0.075) at different Rayleigh numbers.

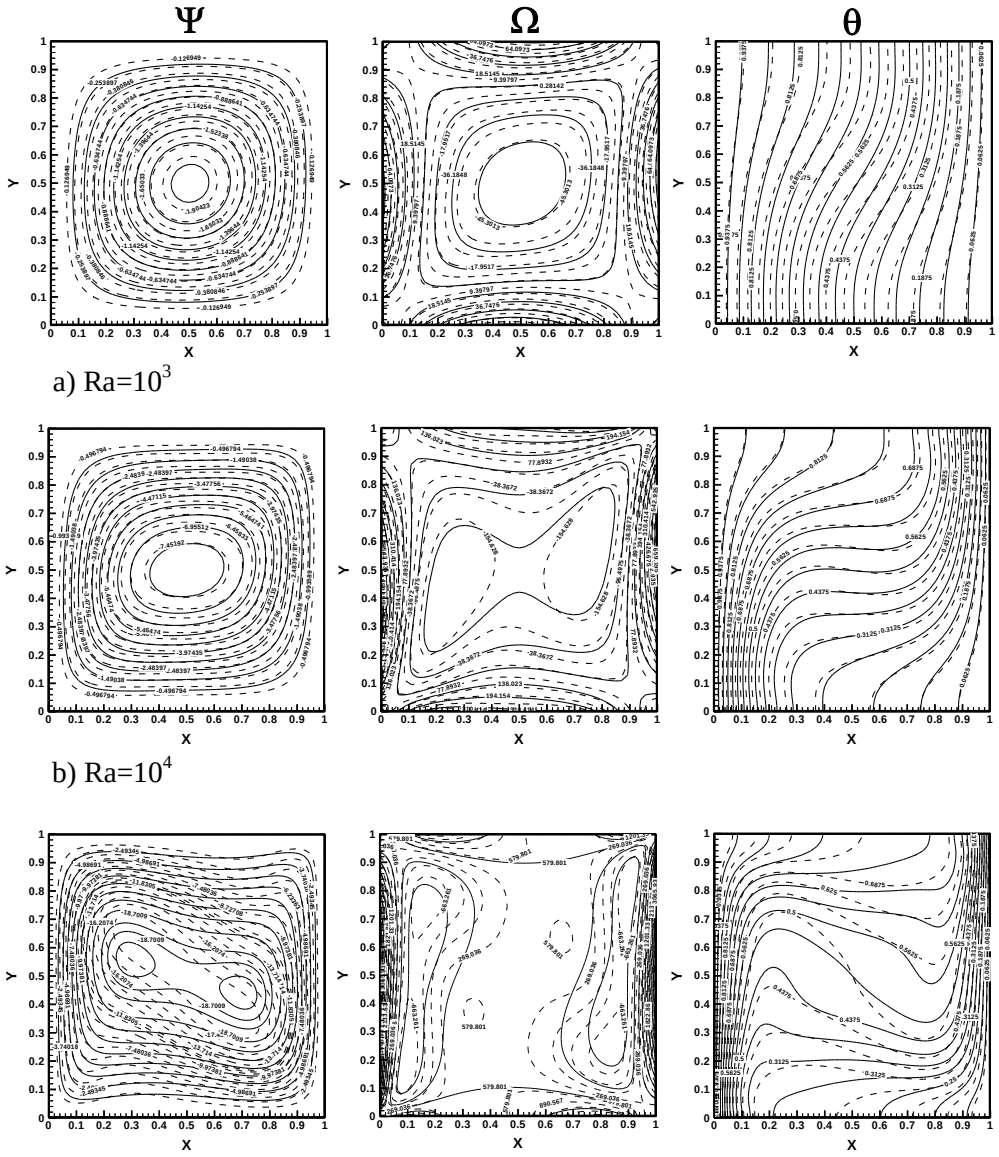

a) Ra=10^3

b) Ra=10^4

c) Ra=10^5

Figure (5): streamlines, vorticity lines and isotherms contours for pure fluid (solid lines) and nanofluids (dash lines) (ϕ=0.1) at different Rayleigh numbers.

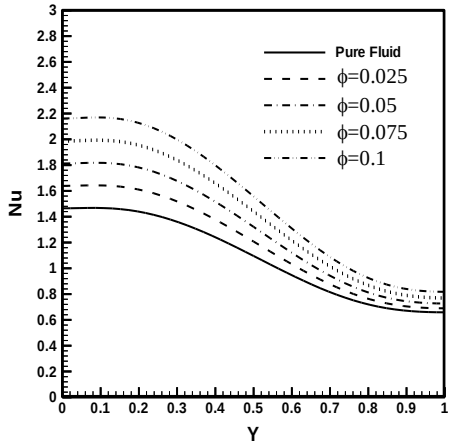

Figure (6): distribution of Nu at Ra=10^3 for pure fluid and nanofluids.

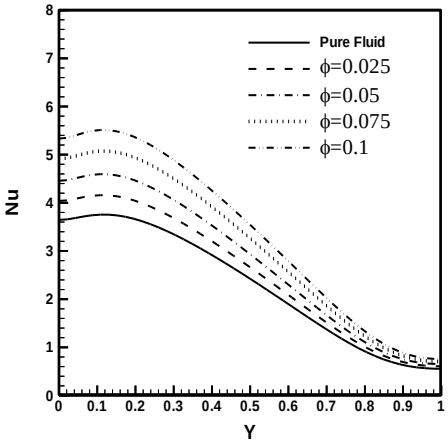

Figure (7): distribution of Nu at Ra=10^4 for pure fluid and nanofluids.

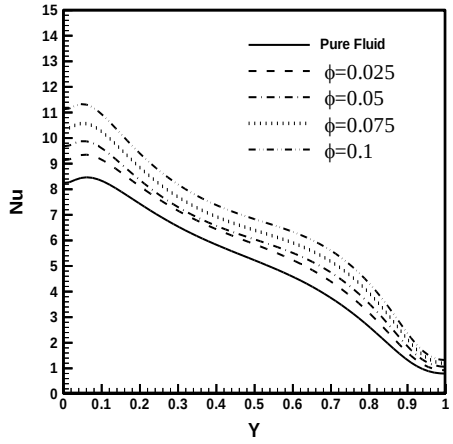

Figure (8): distribution of Nu at Ra=10^5 for pure fluid and nanofluids.

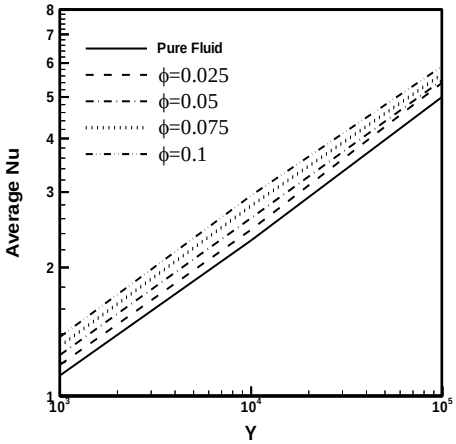

Figure (9): distribution of Nu at Ra=10^3 for pure fluid and nanofluids.

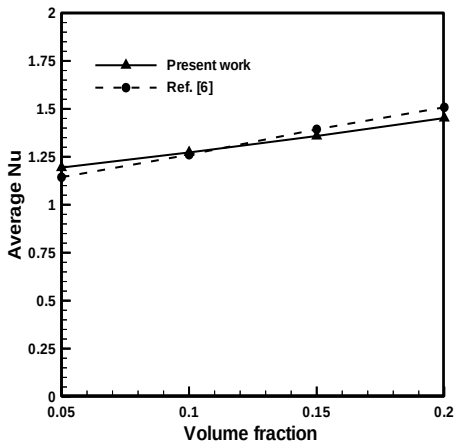

Figure (10): comparison between present work and Ref. [6] for relation between $\overline{Nu}$ and ϕ for Ra=10^3.

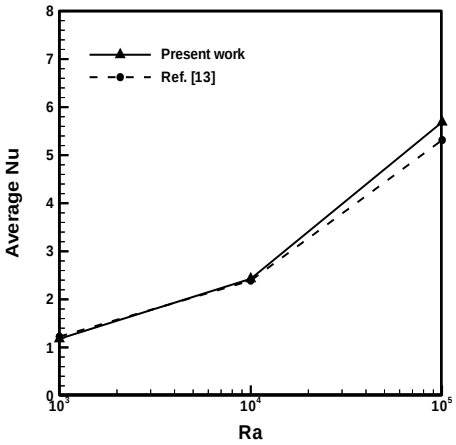

Figure (11): comparison between present work and Ref. [13] for relation between $\overline{Nu}$ and Ra for ϕ=0.04.